

System efficiency of US wind power generation is declining

Peter Regner¹, Katharina Gruber¹, Sebastian Wehrle¹, and Johannes Schmidt¹

¹ *Institute for Sustainable Economic Development, University of Natural Resources and Life Sciences, Vienna*

Abstract

US Wind power generation has grown significantly over the last decades, contributing to the decarbonisation of the US power system. However, the technology also causes negative impacts. Technological progress and choice of locations could, however, decrease these impacts per unit of generated wind power. We assess for the US, which has the second largest wind power fleet globally, how these factors have changed in the period 2010–2019. For that purpose, we combine wind power generation time series, data on installed wind turbines, and wind speed time series to decompose the growth of US wind power generation into its driving factors. We show that wind resources per rotor swept area have increased during the last decade, but system efficiency, i.e. the relation of kinetic power in the wind to wind power generation, has declined stronger. Therefore, less electric power was extracted per rotor swept area in 2019 than 10 years before.

1 Introduction

Globally and in the US, wind power has expanded substantially in recent years. Installed onshore capacity increased from 121 GW in 2008 to 591 GW in 2018 globally [1]. In the US, both installed capacity and generated electricity have nearly tripled since 2010 (see Figure 1). Installed capacity increased from 41 GW in 2010 to 110 GW in 2019. Further growth of the wind power sector is necessary, particularly in light of the stringent mitigation goals until 2030 recently announced by the US [2]. The International Renewable Energy Agency suggests an installed wind power capacity of 857 GW by 2050 for the US in their climate-resilient pathway, which limits global rise in temperature to well below 2 degrees [3, p. 31]. In all decarbonization scenarios, wind power plays a fundamental role in most countries, particularly in Northern latitudes, where solar photovoltaic generation is less competitive as solar irradiation is much lower (see e.g. [4] for the US).

However, wind power expansion has adverse side effects on wildlife, and it is perceived to disturb natural landscapes [5]. Wind turbines are, for instance, known to be hazardous to birds [6] and bats [7]. At the same time, noise, visibility and aesthetics can cause a reduction in living quality [8] and reduce

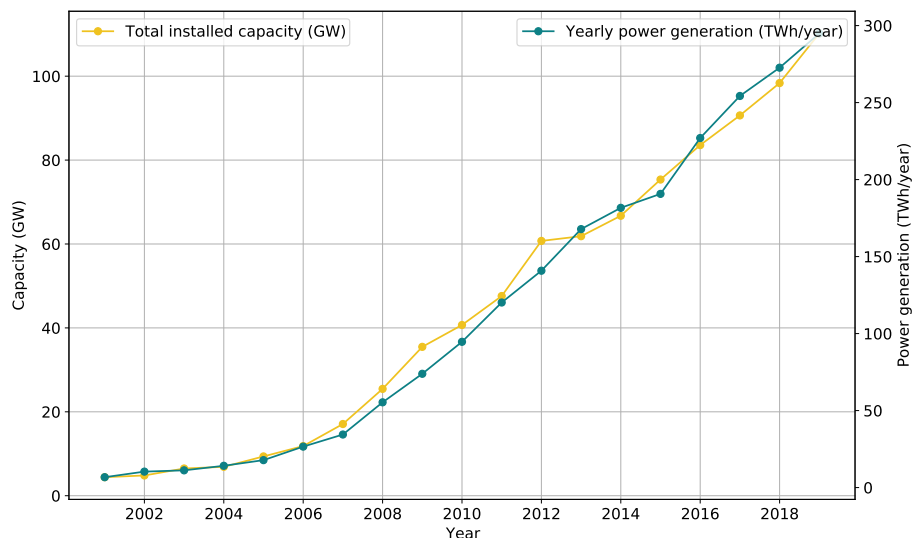


Fig. 1: Growth in installed capacity and annual electricity generation from wind power in the US, 2000–2020.

property prices in proximity to wind parks [9, 10, 11]. The number and the size of operating wind turbines affects the severity of such negative externalities. A growth of rotor diameters leads to an increase in rotor swept area, threatening flying species such as birds and bats. Larger rotors also increase the visibility of wind turbines, as does a growth in hub heights. This will increase impacts on the visual quality of landscapes. For instance, Dröes et al. [9] find that the effect of increasing property prices is stronger for taller turbines. The number of installed wind turbines determines how much land has to be directly converted to host wind parks. However, depending on the wind park management in place, land in-between wind turbines, the so called spacing area, can also be affected [12].

Furthermore, land available for wind power generation is limited – for example, in Bavaria, Germany, legal restrictions regarding minimum distances to residential housing limits the land available for new wind parks to such an extent that a significant expansion of wind power is made impossible [13, 14]. Therefore, the feasible wind power potential may fall short of the optimal capacity derived from power system expansion models, causing additional system costs [15].

One way of minimizing externalities would be to increase the output of turbines without installing additional equipment, i.e. by increasing the output of wind turbines per unit of rotor swept area. If the distance between turbines is proportional to the rotor diameter, then the rotor swept area is also proportional to the spacing area necessary to place wind turbines. Under this assumption,

wind power output per rotor swept area can be used as a measure of impacts on the surroundings similarly to wind power output per area of land (such as in [16, 17]). Increasing the output of wind turbines per unit of rotor swept area can be achieved by increasing the amount of wind flowing through the rotor swept area – or by technological improvements which increase the ratio of kinetic power in the wind to wind power generation. Increasing the amount of wind available to wind turbines is possible by building turbines in windier regions – and by building higher turbines. However, windy locations are of course limited and increasing the hub height of wind turbines will potentially increase externalities of wind power generation, e.g. due to higher visibility. Improving technology, while limited by physical boundaries, may therefore be the only option to increase wind power output without also increasing some externality at the deployment locations of turbines.

Here, we pose therefore the question why wind power output grew historically in the US. In particular, we assess if output per unit of swept rotor area did increase or decrease. Furthermore, we determine how a change in the wind available to turbines and a change in how efficiently kinetic power is converted into wind power contribute to a change in output normalized to rotor swept area. For that purpose, we decompose the growth of the power output of the US wind power fleet into its driving factors, motivated by the formula for wind power output for horizontal-axis wind turbines. In particular, we decompose the change in power output into a change in the number of turbines, in rotor swept area per turbine, in kinetic input power available to turbines, and into system efficiency. Furthermore, we show how the latter two explain the change in power generation per rotor swept area. We further use an additive decomposition approach to show how the kinetic input power available to turbines has changed due to new locations, change in average hub heights, and due to annual variations in wind regimes.

2 Measuring wind power efficiency

Here, we introduce several measures to better understand the technical performance of the US wind power fleet. For a discussion of these measures in comparison to existing ones, see section A.4.3. In the following, we refer to *power input* P_{in} as the total kinetic power of moving air flowing through the rotor swept areas of wind turbines. P_{out} is used to denote the total wind *power output*, i.e. the total generated electric power for all operating wind turbines in the US. The total rotor swept area is called A . First, we define *output power density* as the amount of generated electric power per unit of rotor swept area $\frac{P_{\text{out}}}{A}$. This measure is a combination of power input per rotor swept area, i.e. *input power density*, and of the efficiency of converting that wind into electric power, in the following called *system efficiency*:

$$\frac{P_{\text{out}}}{A} = \frac{P_{\text{in}}}{A} \cdot \frac{P_{\text{out}}}{P_{\text{in}}}. \quad (1)$$

System efficiency denotes the share of power input converted to electricity, i.e. the ratio of power output and power input. System efficiency results from different influencing factors, such as the Betz' limit, mechanical and technical efficiency, curtailing, and downtime due to maintenance, as discussed in more detail in section 3.1.

The same terminology allows for a multiplicative decomposition of wind power output into the total number of operating turbines, average rotor swept area per turbine, input power density, and system efficiency. Denoting the total number of operating turbines with N , the decomposition can be formally described by

$$P_{\text{out}} = N \cdot \frac{A}{N} \cdot \frac{P_{\text{in}}}{A} \cdot \frac{P_{\text{out}}}{P_{\text{in}}} \quad (2)$$

In section A.1, we show how our decomposition is motivated by the physical formula for deriving wind power generation from wind speeds. For each of the variables, a time series will be calculated for the period 2010–2019. P_{in} is computed by estimating the kinetic power in wind for each turbine's location and height on an hourly basis. However, since time series of power output are available only in an aggregated form for the whole US with monthly resolution and commissioning dates for wind turbines are given only with yearly resolution, we defined the variables P_{in} , P_{out} , N , and A as yearly aggregated time series for all wind turbines in the US. That means for T being the set of all hours in a year and L being the set of all turbine locations, the aggregated time series P_{in} is given by

$$P_{\text{in}}(T) = \frac{1}{|T|} \sum_{t \in T} \sum_{l \in L} p_{\text{in}_l}(v_{t,l}), \quad (3)$$

where $p_{\text{in}_l}(v_{t,l})$ is the kinetic power in wind flowing through the rotor swept area at location l at timestamp t (see section A.1).

Similarly, $P_{\text{out}}(T)$ is the average generated electricity in time period T of all wind turbines, but in this case, also system effects are included since $P_{\text{out}}(T)$ is the wind power generated by all turbines and not the theoretical wind power output by a single turbine for a given wind speed. $P_{\text{out}}(T)$, i.e. total wind power generation in the US, is taken from the Energy Information Administration (EIA, see section 5.5.3).

3 Results

Generated electric power per rotor swept area, i.e. the output power density, dropped from 94W/m² in 2010 to 89W/m² in 2019 (Figure 2). This implies

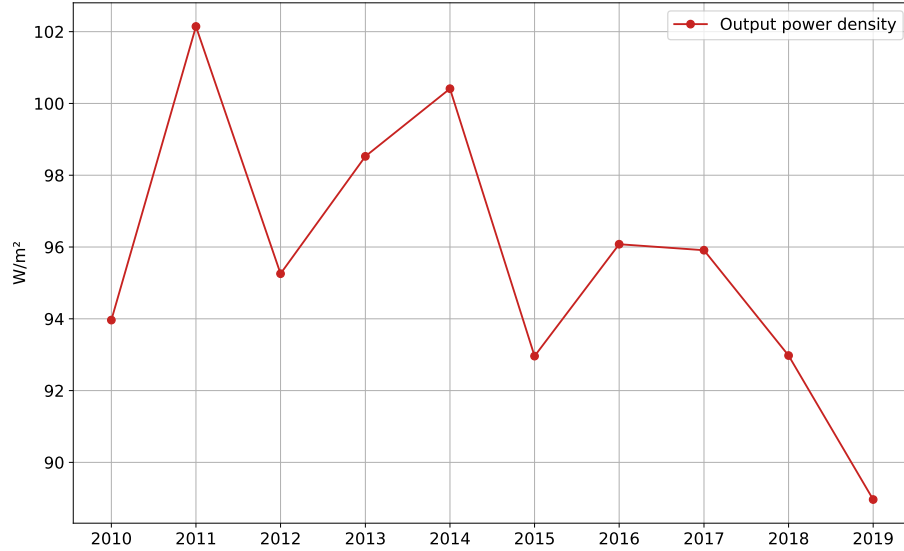


Fig. 2: Power output density $\frac{P_{out}}{A}$: electricity generation per unit of rotor swept area shows strong annual variations and a slight decline in the period 2010–2019.

that in 2019, around 5% less power output was generated per unit of rotor swept area than in 2010. A linear regression of the time trend on output power density shows that the latter decreased by $0.7\text{W}/\text{m}^2$ per year.

Our decomposition approach allows to understand how the declining output power density is explained by a decrease in system efficiency, offset by an increase in input power density. Power output density is the combination of effects in input power density and system efficiency (see equation (1)). The decline of system efficiency since 2010 was stronger than the increase in input power density. A linear regression of a time trend on the change in system efficiency relative to 2010 indicates a decrease of 1.4 percentage points per year, while input power density increases by 0.8 percentage points per year. Hence, the decline of power output density is a result of the lower system efficiency. Trends in system efficiency and power input density are described in more detail in the next subsections.

The decomposition in equation (2) also reveals major drivers of the growth of wind power generation (Figure 3). The change in the number and in the size of turbines are contributing to the growth of power output almost equally. If turbine size had not increased, the number of turbines would have to be almost doubled to achieve the same output level, everything else equal. The factors rotor swept area and the number of operating turbines, are responsible for output growth of 176% and 187%, respectively, in 10 years. The number of turbines has increased from 37,636 in 2010 to 69,975 in 2019. The average rotor

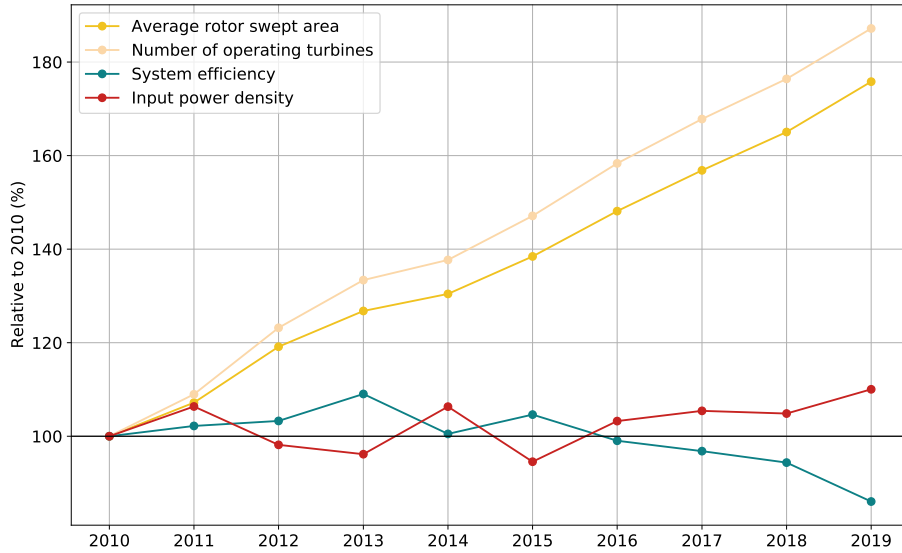


Fig. 3: Driving factors of wind power generation: number and rotor size of turbines are the major drivers for the growth of wind power generation.

swept area of a turbine has increased from $3,179\text{m}^2$ in 2010 to $5,589\text{m}^2$ in 2019, caused by an increase in average rotor length.

3.1 Trends in system efficiency of wind power generation

System efficiency, i.e. the share of power output compared to power input, as presented in equation (2), has declined over the past decade from 38.3% in 2010 to 33.0% in 2019, with substantial variability between years (Figure 4). A linear regression of a time trend on system efficiency shows that there is a decrease of 0.55 percentage points in system efficiency per year.

This variability can be explained by fluctuations in wind conditions between years. In times of low wind speeds, system efficiency tends to increase, while it tends to decrease in years with high wind speeds. The reason is that the efficiency of converting power in the wind into electricity is not uniform over the whole range of wind speeds for wind turbines. For low wind speeds, this conversion efficiency is low, it increases with higher wind speeds and decreases again for very high wind speeds. For the US, we find that relatively low wind speeds move the fleet of wind turbines into a more optimal range of the conversion efficiency, while higher wind speeds tend to move the fleet out of that range. This effect is partly explained by the temporal and spatial aggregation, as high power input or power output values have a larger impact on the average (see section A.4.1). In conclusion, we find that the efficiency of wind turbines declines in wind resource-rich years. Figure A.6 shows the negative correlation

between system efficiency and input power density. The correlation coefficient between monthly aggregated time series of system efficiency and input power density is $R = -0.886$.

However, even under the assumption of constant input power density, a declining trend in system efficiency can be identified. A linear regression model was used to predict a theoretical scenario for the system efficiency in the period 2010–2019, holding input power density constant (see section 5.3). In this scenario, system efficiency declines with a slightly lower slope of -0.27 percentage points per year, from 37.4% to 35.8% (see Figure 4). Therefore, we conclude that the increase of input power density is not the only influencing factor for the decline of system efficiency.

Lower specific power¹ reduces system efficiency, as it increases the share of the input wind power, which is not converted to electricity by wind turbines compared to a turbine with a higher specific power. At the same rotor size, a turbine with a smaller rated capacity but similar slope in its power curve will reach the upper limit of the turbine capacity more often than one with a higher rated capacity – this implies that implicitly, input wind power is curtailed by turbines with a lower specific power. We find that the specific power decreased from 313W/m² to 220W/m² during 2010–2019, which is in accordance with other results [18]. Hence, we conclude that the decline of specific power is one of the reasons for lower system efficiency.

Besides input power density and specific power, other factors can affect system efficiency. However, the limited length of the time series, lack of detailed data, and the high correlation between these factors prevent us from drawing conclusions on their individual contribution to the change in overall system efficiency. Nevertheless, we list them here: a change in system efficiency can also be caused by aging effects of turbines, by a change in average wake effects in wind parks due to changing wind park layouts, by changes in the amount of curtailment of wind energy, by downtime due to maintenance, and by downtime due to extreme weather conditions other than wind speeds such as icing or snow. Finally, the technical efficiency, i.e. losses in the electrical generator and transmission, may also change system efficiency. The latter are losses that can be expected to be lowered by technical progress.

3.2 Trends in input power density

Input power density $\frac{P_{in}}{A}$, the kinetic power in wind per rotor swept area of all operating turbines, depends on the turbine locations and their distribution of wind speeds, the turbines' hub heights, and the climate conditions and its variations. Input power density, as used in the multiplicative decomposition in equation (2), is the result of a combination of annual variations in wind conditions and different trends. We, therefore, applied an additive decomposition to quantify the effects of changes in wind speeds due to new turbine locations, changes in average hub heights, and annual variations (see Figure 5).

¹ Specific power is the ratio between the nameplate capacity, i.e. the size of the generator, and the rotor swept area of a wind turbine.

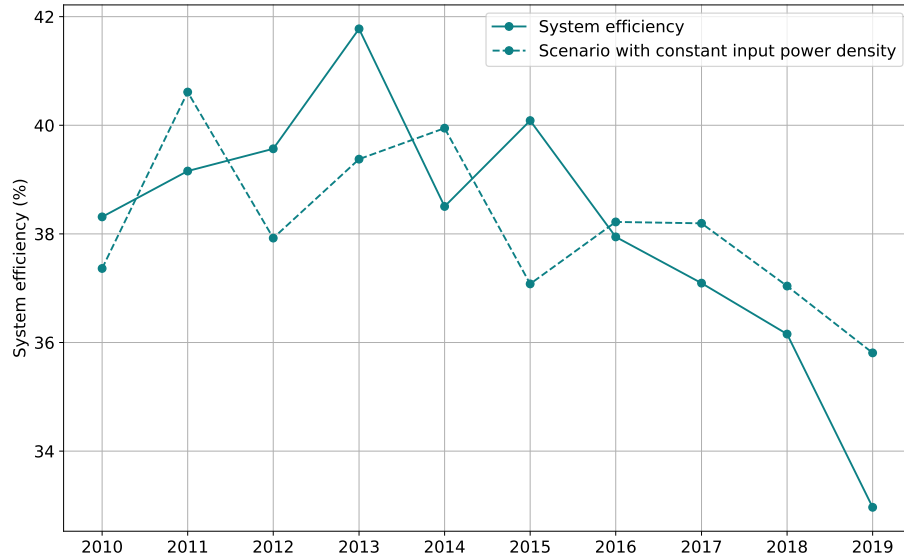


Fig. 4: System efficiency shows a decline in the period 2010–2019. This is partially caused by an increase of input power density, but system efficiency declines also in a scenario under the assumption of constant input power density.

As expected, the growth of average hub heights led to a steady increase in input power density. Since 2010 an increase of $11.4\text{W}/\text{m}^2$ can be attributed to higher wind turbines. Furthermore, since 2013 the deployment of turbines at locations with more wind resources caused the input power density to increase but exceeds the 2010-level only after 2015. Between 2010 and 2013, input power density declined by $8.3\text{W}/\text{m}^2$ due to new locations being less windy than previous ones, but since 2013 it increased by $21.6\text{W}/\text{m}^2$ due to location choice. Changes in input power density due to annual variations of wind conditions are of larger amplitude and range from $-19.5\text{W}/\text{m}^2$ to $17.9\text{W}/\text{m}^2$.

Note that the decomposition does not allow for a perfect decomposition of these three effects. The effect of annual variations amplifies towards the end of the time series due to the growth of hub heights and therefore also higher average wind speeds at hub heights of turbines. More details are described in section 5.4 and the Appendix (see Figure A.5).

4 Discussion

We showed that the growth of wind power generation in the US was driven mainly by increases in the total rotor swept area of operating turbines: the rotor swept area per turbine, and the number of new turbines contributed to output growth similarly. The increase in rotor swept area per turbine has reduced direct

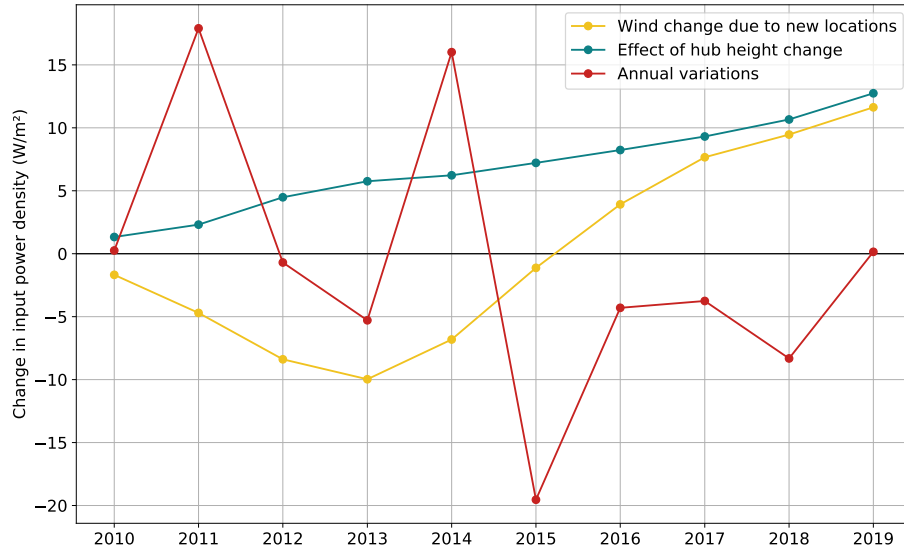


Fig. 5: Decomposition of input power density $\frac{P_{in}}{A}$: turbines were installed at windier locations since 2013 and hub heights led to a steady increase in input power density. As expected, annual variations do not show a clear trend.

impacts on land per generated unit of power, as fewer turbines had to be built. However, the rotor swept area necessary to produce a given output has slightly increased in the last decade. This implies that all related impacts, particularly on wildlife and landscape disturbance, have increased more than power output. In 2019, output per unit of rotor swept area was only 95% of the output in 2010.

Besides being linked to wind power externalities, the rotor swept area also indicates the spacing area necessary in-between turbines, and thus the size of land necessary for the wind park. If the distance between turbines required to reduce wake effects to an acceptable level is proportional to the rotor diameters, the total rotor swept area is also proportional to the spacing area if effects at the borders of wind parks are neglected. A simplified rule of thumb based on rotor sizes is often used to estimate spacing area requirements: it is assumed that a spacing of 7–12 times the rotor diameter in prevailing wind direction and 2–5 times the rotor diameter in the perpendicular direction between wind turbines has to be guaranteed [19, 20, 21, pp. 76–77, 22, p. 423]. Lower distances will increase losses due to wake effects too much. Our results indicate that roughly 5% more wind power could have been generated with the same land requirements per unit of generated electricity if the output power density of wind turbines would have been maintained at the level of 2010.

Higher turbines and more windy locations have allowed to increase the wind available to the rotor swept area of turbines. However, higher turbines also

increase the visibility of turbines and are technically limited. Therefore, significant trade-offs have to be faced when aiming at further increasing hub heights in the future. Windy locations may also become scarce in the future, but we did not assess the geographical patterns of the wind power expansion in detail. Anyhow, a decrease in system efficiency has offset these gains in input power density.

Even if technological progress has likely improved wind turbines and optimizations of wind park layouts may have increased the output of wind parks, our results show that total system efficiency has declined over the last decade. Data does not allow for a definite conclusion, but it can be assumed that one of the main reasons for decreasing system efficiency is the fall in specific power of wind turbines. Of course, there are economic and technical reasons for this fall: less variable output of turbines and relatively little additional cost for building larger rotors makes wind turbines with lower specific power attractive to investors and the power system [18]. If technologies that can integrate variable generation become very cheap and land very scarce, this trend may be reversed in the future. Particularly in land-constrained countries, the situation might be different.

In addition to these empirical results, our analysis also contributes to the discussion on the impacts of wind power expansion by a decomposition that allows distinguishing in detail between the factors contributing to output growth. This complements existing analyzes and indicators and will allow further applications: first, primary energy use of wind power generation can be derived, and the factors which influence its evolution can be understood with our decomposition approach. Second, the method allows to compare the build-out of wind power in different countries consistently, linking power generation to its impacts in terms of turbines built and rotor area swept. There is, therefore, significant potential for future research using our approach.

5 Methods & Data

In the following sections, details about the computation of the presented results and used data sets are described. Used code is published under the MIT license on Github² and can be used to reproduce the results.

5.1 Computation of power input

In a first step, wind velocities at 10m and 100m at the precise turbine location were estimated from raw ERA5 data (see section 5.5.1) using bilinear interpolation in the directions of longitude and latitude. Directionless wind speeds were then computed from u and v components for each turbine location l and time stamp t .

Subsequently, the wind power law $v_h = v_{h_0} \cdot \left(\frac{h}{h_0}\right)^\alpha$ was applied to estimate

² <https://github.com/inwe-boku/windpower-decomposition-usa>

the wind speed at different heights h by computing

$$\alpha = \log_{\frac{100\text{m}}{10\text{m}}} \left(\frac{v_{100\text{m}}}{v_{10\text{m}}} \right)$$

for each turbine location and time stamp and then calculate v_h with $h_0 = 100\text{m}$.

To compute P_{in} , we apply the formula $p_{\text{in}_l}(v_{t,l}) = \frac{1}{2}\rho A_l v_{t,l}^3$ using wind speed $v_{t,l}$ at hub height to compute the input power at turbine location l at time t . P_{in} is then the yearly aggregated time series for all turbine locations L

$$P_{\text{in}}(T) = \frac{1}{|T|} \sum_{t \in T} \sum_{l \in L} p_{\text{in}_l}(v_{t,l}),$$

where T is the set of hourly timestamps for each year (see also equation (3)).

5.2 Computation of total rotor swept area and number of operating turbines

Time series for the total rotor swept area A , and number N of operating turbines are derived from the United States Wind Turbine Database (USWTDB). After removing all turbines from the data set, where the commissioning year is missing, mean data imputation for each commissioning year was used to estimate missing values for the rotor diameter parameter (see section 5.5.2). The rotor diameter was then used to calculate the rotor swept area A_l for each turbine at location l . To compute a time series, the sum of the rotor swept areas of all operating turbines was calculated for each year.

The commissioning date is given only with a yearly resolution. Therefore a weight of 0.5 is used for turbines in their commissioning year when summing up rotor swept areas of operating turbines and the number of turbines. This is motivated by the assumption that turbines are built with equal probability throughout the year, so on average, they contribute only 50% to the aggregated value in the first year.

5.3 Analysis of trends in system efficiency

To analyze whether the decline in system efficiency is caused only by an increase of input power density, we apply the following linear regression model

$$E(t) = \alpha_1 \cdot D_{\text{in}}(t) + \alpha_0 + \epsilon(t),$$

where $E = \frac{P_{\text{out}}}{P_{\text{in}}}$ is the system efficiency and $D_{\text{in}} = \frac{P_{\text{in}}}{A}$ is the input power density, both with yearly resolution. We then apply the average input power density $\overline{D_{\text{in}}}$ to the model

$$\hat{E}(t) = \alpha_1 \cdot \overline{D_{\text{in}}} + \alpha_0 + \epsilon(t).$$

to estimate a scenario with constant input power density.

5.4 Decomposition of input power density

Input power density $\frac{P_{\text{in}}}{A}$ is subject to large climatic variations. An additive decomposition is used to observe underlying trends unrelated to the climate. In the following, we describe the decomposition in more detail.

Note that input power density $\frac{P_{\text{in}}}{A}$ is proportional to the weighted average of $v_{t,l}^3$ with weights A_l , because a constant value is used for the air density ρ . Therefore, input power density changes, if wind speeds $v_{t,l}$ change.

The average wind speed at the hub height at turbine locations changes because of turbines being added at new locations, a change of the average hub height, or a change of climate conditions (either annual or multi-annual variability or trends due to, e.g. climate change). In order to analyze these different components, power input will be computed under different hypothetical conditions. $P_{\text{in},76\text{m,avg}}$ is the power input at turbine locations at a baseline height of 76m using average power input over the entire period. $P_{\text{in,avg}}$ is the total input power at all turbine locations at the hub height of installed turbines when also assuming average climate conditions. P_{in} is the actual input power captured by all installed wind turbines (see section 5.1). These definitions can be used for the following decomposition:

$$\begin{aligned}
 P_{\text{in}} &= && \text{baseline} \\
 &+ && P_{\text{in},76\text{m,avg}} - \text{baseline} && \leftarrow \text{effect of new locations} \\
 &+ && P_{\text{in,avg}} - P_{\text{in},76\text{m,avg}} && \leftarrow \text{hub height change} \\
 &+ && P_{\text{in}} - P_{\text{in,avg}} && \leftarrow \text{annual variations of climate conditions}
 \end{aligned}$$

The baseline is an arbitrary value. It is chosen in a way, such that the effect of new locations is zero in the first year of the considered period. Similarly, the baseline height of 76m is chosen, such that the effect of hub height change is close to zero in the first year. To get an additive decomposition of the input power density $\frac{P_{\text{in}}}{A}$, we divide the equation on both sides by A . This allows quantifying the effect of changes in wind speeds due to new locations, the effect of change in hub heights and the effect of annual variations in available wind resources.

Note that the annual variations of climate conditions is not independent of the effect of hub height change. Average wind speeds at hub height are increasing over time, since average hub heights of new turbines are increasing over time and average wind speeds are higher at larger heights. Therefore also the difference $P_{\text{in}} - P_{\text{in,avg}}$ exhibits larger variations over time, when compared with variations of input wind power at the same heights.

A graphical explanation of the additive decomposition of input power density is illustrated in the Appendix in Figure A.5.

5.5 Data

We aimed at mainly using publicly available data sets to compute the presented results. However, the turbine data set was extended by non-public data as

explained in section 5.5.2 in more detail. External input data were validated using additional data sets as described in the Appendix in section A.2.

5.5.1 Wind speed data

To estimate the power input at turbine locations, wind speeds from the ERA5 data set [23] were used. ERA5 is an openly available global reanalysis data set. Wind velocities are provided at 10m and 100m height with hourly temporal resolution and 0.25° spatial resolution – in the US this results in tiles with a size of approximately $25\text{km} \times 25\text{km}$.

A previous validation showed that the ERA5 data set can be used to simulate the US wind power output with good accuracy [24]. It was further shown that bias correction with the higher resolved Global Wind Atlas does not reduce the simulation error significantly. Therefore raw ERA5 data were used to compute the time series of input power P_{in} .

5.5.2 Wind turbine data

The United States Wind Turbine Database [25] is a collection of about 70 thousand wind turbines located in the USA. Every turbine is annotated with a precise location, i.e. longitude and latitude, and several other meta parameters such as hub height, rotor diameter, capacity, model name and commissioning year.

However, many of the meta parameters are missing. For 18.1% of the turbines in the data set, there is no hub height or no rotor diameter available. Simply discarding turbines with missing data would lead to a significant underestimation of aggregated values such as the total rotor swept area of operating turbines, which is essential in most parts of the computation. Instead, we used mean data imputation for each year to estimate values for the missing meta parameters for hub height, rotor diameter and capacity. The parameters are missing not at random (MNAR), as there are more missing parameters for older turbines (see section A.2.1). The distribution of missing parameters for turbines built in the same year is unknown, which is why there is no way to find an optimal way of estimating missing values. However, computation of minimum and maximum introduced error – similar to a sensitivity analysis – shows that the introduced error can be neglected.

The public USWTDB data set contains currently operating wind turbines only. This study aims to analyze the historical development of turbines, which naturally requires also knowledge about decommissioned turbines. Via personal communication, we received an extension to the USWTDB data set [26], which consists of turbines that have been removed from the USWTDB by now due to their decommissioning. These turbines have been merged with the publicly available data set.

For some of the turbines in the data set, the commissioning year is missing. These turbines cannot be used in the calculation of the time series and are therefore removed in a preprocessing step. This affects 2.7% of all turbines or 5.2% of turbines operating in 2010. We assume that these are mostly older and

therefore smaller turbines, since the share of turbines without meta parameters is higher for the ones with commissioning year before 2010 (see section A.2.1). Therefore, the discarded total capacity can be assumed to be below 2.7% of the total capacity or below 5.2% relative to capacity installed in 2010.

Decommissioning dates are missing for most turbines. For only 1,718 turbines a decommissioning year is available, but 7,969 turbines are marked as decommissioned and further 4,159 turbines were older than 25 years in 2019. However, since this affects mostly smaller turbines, the effect on the total installed capacity is quite small (see section A.2.2). Therefore, all turbines were used without taking decommissioning into account.

One turbine with a capacity of 275KW located on the Mariana Islands has been removed from the data set because it significantly reduces the size of the bounding box of turbine locations and, therefore, also the size of required wind speed data.

5.5.3 Wind power generation data

Wind power generation time series are provided by the Energy Information Administration [27]. This data set provides monthly and nationwide aggregated time series, which is directly used in our decomposition denoted by P_{out} .

6 Data availability

Data sets required to reproduce all results and figures are described in section 5. The Code Github repository contains download scripts to download the data sets. Only the extension of the USWTDB with decommissioned turbines [26] is non-public and will be made available to readers upon request. Similar results can be reproduced also with the publicly available data sets.

7 Code availability

All developed source code will be published on Github and archived on Zenodo upon publication of the article. Used third party libraries are widely used OpenSource packages, which are freely available. The precise versions used are defined in a Conda environment.

Acknowledgments. We gratefully acknowledge support from the European Research Council (reFUEL ERC-2017-STG 758149). Furthermore we would like to thank Joseph Rand and Ben Hoen for providing data on decommissioned turbines.

Symbols

ρ	air density, constant value of 1.225kg/m^3 is used
P_{in}	power input of all turbines (at hub height)
$P_{\text{in},76\text{m,avg}}$	Wind power at 76m assuming long-term average power
$P_{\text{in,avg}}$	Wind power at hub heights assuming long-term average power
P_{out}	power output of all turbines
N	number of operating turbines
A_l	rotor swept area of a single turbine at location l , i.e. $A_l = \pi \cdot \frac{d_l^2}{4}$ for a turbine with rotor diameter d_l
A	total rotor swept area of all turbines L , i.e. $A = \sum_{l \in L} A_l$
A_{land}	total area of land used in wind parks
L	set of all turbine locations
l	location of a single wind turbine
v	wind speed
$v_{t,l}$	wind speed at location l at time t (at hub height)
$C_p(v)$	coefficient of power, ratio of power output and power input at wind speed v for a specific turbine
T	set of time stamps t for a certain period, i.e. all hours in a year or month
$p_{\text{in}_l}(v)$	power input at wind speed v for turbine at location l with rotor swept area A_l , i.e. $p_{\text{in}_l}(v) = \frac{1}{2}\rho A_l v^3$
$p_{\text{out}_l}(v)$	power output at wind speed v for turbine at location l with rotor swept area A_l , i.e. $p_{\text{out}_l}(v) = \frac{1}{2}\rho A_l v^3 C_p(v)$

References

- [1] Karing Ohlenforst. *Global Wind Report 2018*. Tech. rep. Global Wind Energy Council, 2019. URL: https://gwec.net/wp-content/uploads/2020/02/Annual-Wind-Report_digital_full-1.pdf.

-
- [2] *FACT SHEET: President Biden Sets 2030 Greenhouse Gas Pollution Reduction Target Aimed at Creating Good-Paying Union Jobs and Securing U.S. Leadership on Clean Energy Technologies*. The White House. Apr. 22, 2021. URL: <https://www.whitehouse.gov/briefing-room/statements-releases/2021/04/22/fact-sheet-president-biden-sets-2030-greenhouse-gas-pollution-reduction-target-aimed-at-creating-good-paying-union-jobs-and-securing-u-s-leadership-on-clean-energy-technologies/> (visited on 04/29/2021).
- [3] IRENA. *Future of wind: Deployment, investment, technology, grid integration and socio-economic aspects (A Global Energy Transformation paper)*. Abu Dhabi: International Renewable Energy Agency, 2019.
- [4] Trieu Mai et al. “Renewable Electricity Futures for the United States”. In: *IEEE Transactions on Sustainable Energy* 5.2 (Apr. 2014), pp. 372–378. DOI: 10.1109/TSTE.2013.2290472.
- [5] R. Spielhofer et al. “Physiological and behavioral reactions to renewable energy systems in various landscape types”. In: *Renewable and Sustainable Energy Reviews* 135 (Jan. 1, 2021), p. 110410. DOI: 10.1016/j.rser.2020.110410.
- [6] Ana Teresa Marques et al. “Understanding bird collisions at wind farms: An updated review on the causes and possible mitigation strategies”. In: *Biological Conservation* 179 (2014), pp. 40–52. DOI: <https://doi.org/10.1016/j.biocon.2014.08.017>.
- [7] Jens Rydell et al. “Bat Mortality at Wind Turbines in Northwestern Europe”. In: *Acta Chiropterologica* 12.2 (Dec. 2010), pp. 261–274. DOI: 10.3161/150811010X537846.
- [8] Ian D. Bishop and David R. Miller. “Visual assessment of off-shore wind turbines: The influence of distance, contrast, movement and social variables”. In: *Renewable Energy* 32.5 (Apr. 1, 2007), pp. 814–831. DOI: 10.1016/j.renene.2006.03.009.
- [9] Martijn I. Dröes and Hans R. A. Koster. “Renewable energy and negative externalities: The effect of wind turbines on house prices”. In: *Journal of Urban Economics* 96 (Nov. 1, 2016), pp. 121–141. DOI: 10.1016/j.jue.2016.09.001.
- [10] Cathrine Ulla Jensen et al. “The impact of on-shore and off-shore wind turbine farms on property prices”. In: *Energy Policy* 116 (May 1, 2018), pp. 50–59. DOI: 10.1016/j.enpol.2018.01.046.
- [11] Richard J. Vyn. “Property Value Impacts of Wind Turbines and the Influence of Attitudes toward Wind Energy”. In: *Land Economics* 94.4 (Nov. 1, 2018), pp. 496–516. DOI: 10.3368/le.94.4.496.
- [12] Olga Turkovska et al. “Land-use impacts of Brazilian wind power expansion”. In: *Environmental Research Letters* 16.2 (Jan. 2021), p. 024010. DOI: 10.1088/1748-9326/abd12f.

- [13] Katja Bunzel et al. “Hidden outlaws in the forest? A legal and spatial analysis of onshore wind energy in Germany”. In: *Energy Research & Social Science* 55 (2019), pp. 14–25. DOI: <https://doi.org/10.1016/j.erss.2019.04.009>.
- [14] Nina Hehn and Manfred Miosga. “Die Zukunft der Windenergie in Bayern nach Einführung der 10 H-Regel”. In: *Ausbaukontroverse Windenergie* (2015). URL: <https://eref.uni-bayreuth.de/id/eprint/49276>.
- [15] Sebastian Wehrle, Johannes Schmidt, and Christian Mikovits. “The Cost of Undisturbed Landscapes”. arXiv: 2006.08009. June 2020. URL: <http://arxiv.org/abs/2006.08009>.
- [16] Lee M. Miller and David W. Keith. “Observation-based solar and wind power capacity factors and power densities”. In: *Environmental Research Letters* 13.10 (Oct. 2018), p. 104008. DOI: 10.1088/1748-9326/aae102.
- [17] Lee M. Miller and David W. Keith. “Corrigendum: Observation-based solar and wind power capacity factors and power densities (2018 Environ. Res. Lett. 13 104008)”. In: *Environmental Research Letters* 14.7 (July 2019), p. 079501. DOI: 10.1088/1748-9326/aaf9cf.
- [18] Mark Bolinger et al. “Opportunities for and challenges to further reductions in the “specific power” rating of wind turbines installed in the United States”. In: *Wind Engineering* (Jan. 2020). DOI: 10.1177/0309524X19901012.
- [19] Erkkka Rinne et al. “Effects of turbine technology and land use on wind power resource potential”. In: *Nature Energy* 3.6 (June 2018), p. 494. DOI: 10.1038/s41560-018-0137-9.
- [20] David Ryberg et al. “The Future of European Onshore Wind Energy Potential: Detailed Distribution and Simulation of Advanced Turbine Designs”. In: (Dec. 18, 2018). DOI: 10.20944/preprints201812.0196.v1.
- [21] Mukund R. Patel. *Wind and solar power systems: design, analysis, and operation*. 2nd ed. Boca Raton, FL: Taylor & Francis, 2006. 448 pp. ISBN: 978-0-8493-1570-1.
- [22] James F Manwell, Jon G McGowan, and Anthony L Rogers. *Wind energy explained: theory, design and application*. John Wiley & Sons, 2010.
- [23] H. Hersbach et al. “ERA5 hourly data on single levels from 1979 to present”. In: *Copernicus Climate Change Service (C3S) Climate Data Store (CDS)* (2018). DOI: 10.24381/cds.adbb2d47. (Visited on 11/17/2020).
- [24] Katharina Gruber et al. “Towards global validation of wind power simulations: A multi-country assessment of wind power simulation from MERRA-2 and ERA-5 reanalyses bias-corrected with the Global Wind Atlas”. In: *Energy* (2021), p. 121520. DOI: <https://doi.org/10.1016/j.energy.2021.121520>.
- [25] B.D. Hoen et al. *United States Wind Turbine Database (ver. 3.0, April 2020)*. U.S. Geological Survey, American Wind Energy Association, and Lawrence Berkeley National Laboratory data release. 2018. DOI: <https://doi.org/10.5066/F7TX3DN0>.

- [26] Joseph Rand. personal communication. Mar. 26, 2020.
- [27] U.S. Energy Information Administration. *Electricity Open Data*. 2020. URL: <https://www.eia.gov/opa/data/> (visited on 02/20/2020).
- [28] Désiré Le gourières. “CHAPTER V - DESCRIPTION AND PERFORMANCES OF VERTICAL AXIS WINDMILLS”. In: *Wind Power Plants*. Ed. by Désiré Le gourières. Pergamon, Jan. 1, 1982, pp. 121–147. ISBN: 978-0-08-029966-2. DOI: 10.1016/B978-0-08-029966-2.50011-0.
- [29] International Renewable Energy Agency (IRENA). *Query Tool*. URL: <https://www.irena.org/Statistics/Download-Data> (visited on 02/26/2020).
- [30] Ryan Wisser et al. “2018 Wind Technologies Market Report”. In: (2019), p. 103.
- [31] IRENA. *Renewable power generation costs in 2019*. Abu Dhabi: International Renewable Energy Agency, 2020. ISBN: 978-92-9260-244-4.
- [32] Lisa Ziegler et al. “Lifetime extension of onshore wind turbines: A review covering Germany, Spain, Denmark, and the UK”. In: *Renewable and Sustainable Energy Reviews* 82 (Feb. 1, 2018), pp. 1261–1271. DOI: 10.1016/j.rser.2017.09.100.
- [33] International Renewable Energy Agency (IRENA). *Wind Energy Data*. URL: <https://www.irena.org/wind> (visited on 09/07/2020).
- [34] Alain Ulazia et al. “Global estimations of wind energy potential considering seasonal air density changes”. In: *Energy* 187 (Nov. 15, 2019), p. 115938. DOI: 10.1016/j.energy.2019.115938.

A Appendix

A.1 Motivation of decomposition

Our decomposition

$$P_{\text{out}} = N \cdot \frac{A}{N} \cdot \frac{P_{\text{in}}}{A} \cdot \frac{P_{\text{out}}}{P_{\text{in}}}$$

is motivated by the generic formula describing the relationship between wind available to turbines and wind power generation:

$$p_{\text{out}_l}(v) = \frac{1}{2} \rho A_l v^3 C_p(v).$$

The wind power output of a single wind turbine $p_{\text{out}_l}(v)$ is proportional to the rotor swept area A_l , to the cube of the wind speed v and to the air density ρ . Here A_l denotes the rotor swept area of a single wind turbine at location l and should not be confused with the total rotor swept area A of all operating turbines. The share of wind power converted to electricity is typically denoted by $C_p(v)$ and called the coefficient of power (see, e.g. [28]). $C_p(v)$ describes how efficiently a turbine can convert wind power to electricity at wind speed v .

Input wind power at wind speed v is given by $p_{\text{in}_l}(v) = \frac{1}{2}\rho A_l v^3$, so that the coefficient of power can be written as the ratio of power output to power input

$$C_p(v) = \frac{p_{\text{out}_l}(v)}{p_{\text{in}_l}(v)}.$$

An upper bound to $C_p(v)$ is given by Betz' limit. For a single turbine, the function $p_{\text{out}_l}(v)$ is usually called power curve, where A_l depends on the rotor diameter of the turbine model, v is the wind speed at hub height and $C_p(v)$ combines all other turbine specific characteristics. Air density ρ depends on climate conditions, weather and locations [34], but in practice, a constant value is typically used for power curves and also in our analysis. Here we use $\rho = 1.225\text{kg/m}^3$. That means that rotor swept area A_l , the cube of wind speed v^3 and efficiency $C_p(v)$ are the only non-constant parts in $p_{\text{out}_l}(v)$. Also note that $p_{\text{in}_l}(v)/A_l$ is proportional to v^3 . This motivates the decomposition of power output into total rotor swept area, system efficiency and input power density as shown in equation (2). Total rotor swept area is further decomposed into the number of operating turbines N and the average rotor swept area per turbine $\frac{A}{N}$.

Our definition of system efficiency $\frac{P_{\text{out}}}{P_{\text{in}}}$ includes curtailing, wake effects and other losses. This is in contrast to the coefficient of power whereas $C_p(v)$ takes only mechanical, electrical or aerodynamic losses caused by a single turbine into account (see section 3.1 for more details). However, system efficiency is the relevant measure to analyze the change in the total growth of wind power generation and its impacts.

A.2 Validation

We compared the data used in our analysis to different, independent sources in order to gain confidence in its validity. The following subsections describe how missing data was estimated and why we are confident that the introduced errors are minor.

Figure A.1 provides an overview of comparisons. Four different sources are compared. Wind power output computed using ERA5, USWTDB and power curves in [24] are compared to the monthly power output reported by the EIA [27]. The RSME between monthly capacity factors was found to be 0.031 [24]. This increases our confidence that ERA5 data is able to represent wind conditions at wind turbine sites well. Annual wind power output from the EIA data set is also compared to wind power output provided by IRENA [33]. A maximum relative deviation of 1.2% was identified (Figure A.2). Installed capacity calculated from the USWTDB data set deviates less than 5% from installed capacity reported by the IRENA data set when comparing yearly time series in the period 2010–2019 (see section A.2.2). Specific power calculated from the USWTDB is in accordance with the data reported in [30].

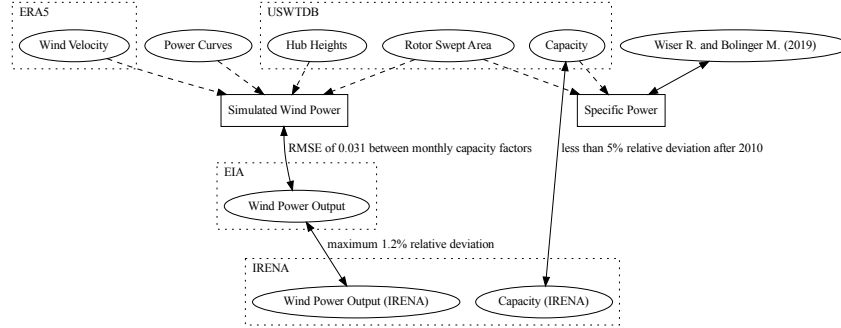


Fig. A.1: Overview of validation between different data sources.

A.2.1 Missing meta parameters

The USWTDB provides a list of all operating wind turbines in the US. However, meta parameters such as rotor diameter, hub height or capacity are missing for many turbines. Figure A.3 shows the share of missing meta parameters of turbines installed in a certain year. Missing meta parameters are estimated using mean data imputation for turbines with the same commissioning date. Meta parameters are missing mostly for older turbines. In the period 2000–2010, the share of operating turbines, where no value for capacity is available in the USWTDB, drops from 26% to 10%. After 2010, we see also a higher match between the total installed capacity reported by the USWTDB (using mean data imputation) and IRENA (see section A.2.2).

A.2.2 Validation with IRENA

Missing turbines in the USWTDB would lead to an underestimation of P_{in} and subsequently to an overestimation of system efficiency. Therefore, we compared the USWTDB to a second data source. The IRENA Query Tool [29] provides the yearly installed wind power capacity per country and technology. Figure A.4 shows the relative difference of installed wind power capacity between the two data sources IRENA and USWTDB. Installed capacity was derived for different scenarios from the USWTDB. The yellow line shows the installed capacity excluding turbines marked as decommissioned. Since most decommissioning dates are not available in the data set, in this scenario, all turbines marked as decommissioned are removed for the complete timespan. The red line indicates the capacity of all installed turbines neglecting decommissioning of turbines. All other solid lines illustrate scenarios under different assumptions of turbine lifetime while ignoring whether the turbines are marked as decommissioned in the database.

As explained in section A.2.1, in the USWTDB meta parameters are missing

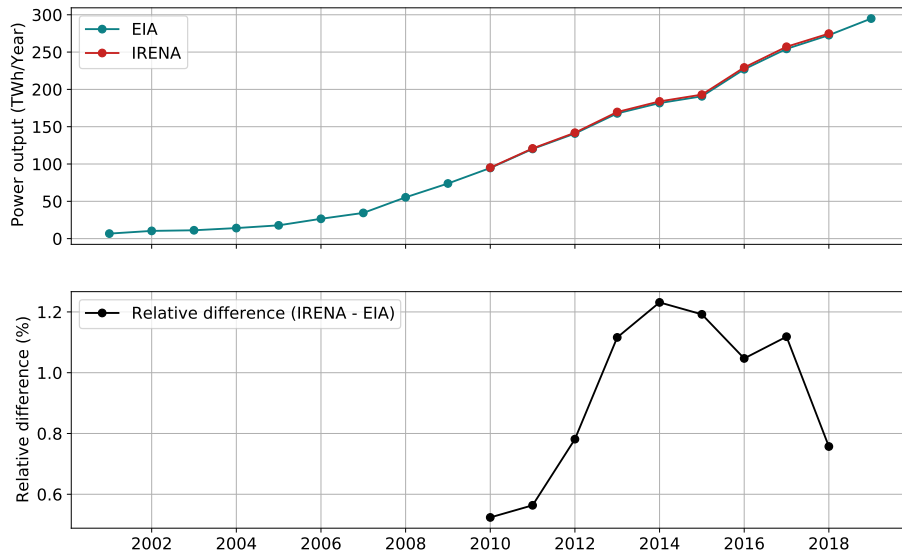


Fig. A.2: Comparison of two independent data sets reporting wind power output in the US: The data set provided by IRENA shows slightly higher values in comparison to the data set by the EIA.

for many turbines. To estimate a capacity for these turbines, mean data imputation for turbines with the same commissioning year was used. The results are shown in solid lines. In contrast, the dashed lines in Figure A.4 show scenarios, where turbines with unavailable capacity values were simply discarded. Turbines where no commissioning year is available, were removed in all scenarios (see also section 5.5.2).

In the years from 2000–2010, there is a large deviation in installed capacity between USWTDB and IRENA in all scenarios. In the scenario where no turbines are removed due to decommissioning or in the scenario with lifetimes above 20 years, using the USWTDB results in higher installed capacity compared to the IRENA data set. Typical wind turbine lifetimes are not below 20 years [32], we therefore assume that data is missing in the IRENA data set and data before 2010 cannot be used to draw conclusions with reasonable accuracy.

After the year 2010, the deviation between data sets and different scenarios is quite small. We therefore limit our analysis to the period 2010–2019.

A.3 Additive decomposition of input power density

Figure A.5 illustrates the additive decomposition explained in section 3.2 and in section 5.4. The black lines show input power density in different scenarios. The colored bars show the derived effects of wind change due to new locations, of hub height changes and annual variations. The computed input power density

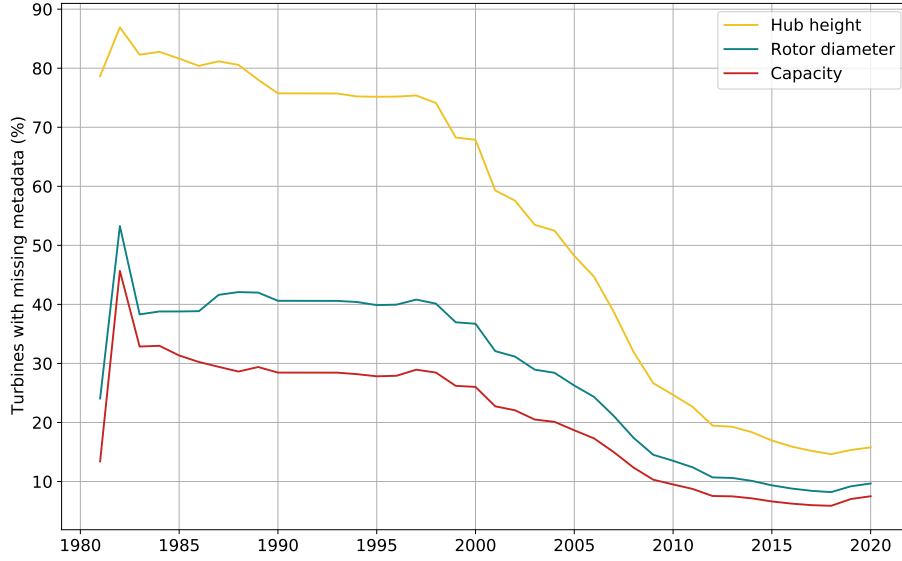


Fig. A.3: Missing metaparameters in the USWTDB of operating turbines. Decommissioning of turbines is neglected.

is the sum of effects and the base line.

A.4 Efficiency

A.4.1 Side effects of calculations with ratios of aggregated time series

System efficiency was defined as the ratio of power output and power input $\frac{P_{out}}{P_{in}}$. Since P_{in} and P_{out} are temporally and spatially aggregated time series, each data point in the time series of system efficiency is a ratio of averages. System efficiency is not identical with the average coefficient of power

$$\overline{C_p} = \sum_{l \in L} \sum_{t \in T} \frac{p_{out_l}(v_{t,l})}{p_{in_l}(v_{t,l})},$$

because in general the ratio of averages does not equal the average of ratios. The ratio of averages is a weighted average of ratios, where each summand is weighted by the denominator

$$\frac{\frac{1}{n} \sum_{i=1}^n a_i}{\frac{1}{n} \sum_{i=1}^n b_i} = \frac{1}{n} \sum_{i=1}^n \frac{b_i}{\frac{1}{n} \sum_{j=1}^n b_j} \frac{a_i}{b_i}.$$

This means that hours with high power input contribute more to the aggregated value of system efficiency. Hence, the average coefficient of power $\overline{C_p}$ and $\frac{P_{out}}{P_{in}}$ are different measures of wind power efficiency. A comparison is discussed in section A.4.3.

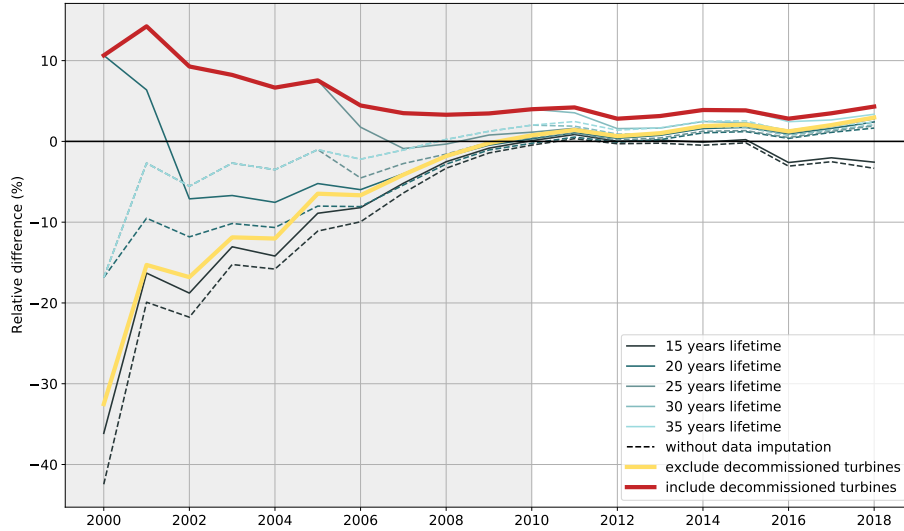


Fig. A.4: Comparison of installed wind power capacity data as provided by the USWTDB and IRENA. A positive value indicates that USWTDB reports a higher value for installed wind power capacity.

A.4.2 Correlation between system efficiency and input power density

Empirical data show a strong negative correlation between input power density and system efficiency (see Figure A.6). This is the result of the efficiency of each turbine $C_p(v)$ for different wind speeds v , the distribution of wind speeds at each turbine location and the spatial and temporal aggregation of P_{out} , P_{in} and A .

The efficiency of a single wind turbine is typically lower at low and high wind speeds. At low wind speeds, there are more losses relative to generated electricity. At high wind speeds, the power output is limited by the size of the generator, i.e. by the nameplate capacity. Compared to the curve of C_p , the monthly aggregated efficiency for one turbine is slightly shifted due to the asymmetry of wind speed distributions. In locations with high mean wind speeds, the declining interval of C_p is dominant and therefore monthly aggregated efficiency is negatively correlated with input power density. Due to the aggregation, locations with high wind speeds have a higher impact on the spatially and temporal aggregated value of system efficiency (see section A.4.1). Therefore system efficiency is negatively correlated to input power density.

A.4.3 Alternative definitions of efficiency

In general, efficiency is the relation between output and input. We defined system efficiency as ratio between total yearly power output to power input. However, this is not the only relevant measure of wind power efficiency. Instead

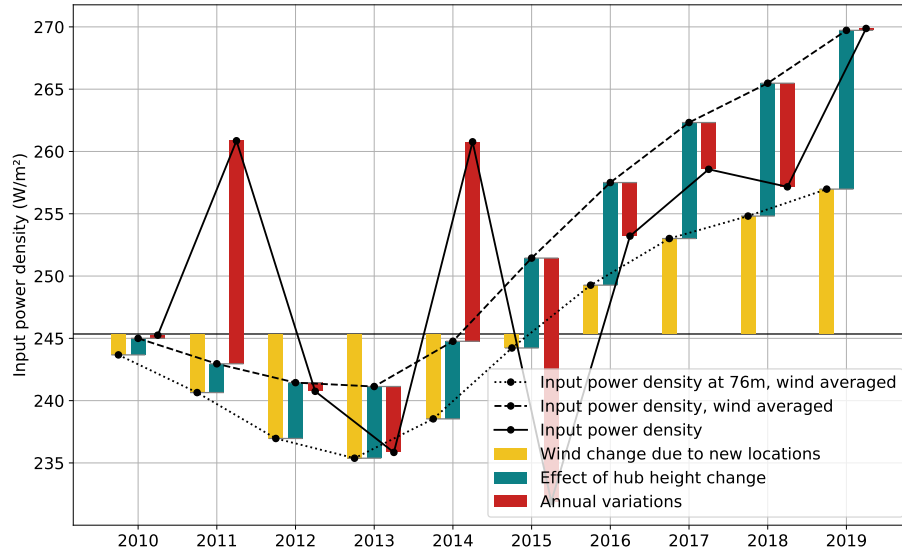


Fig. A.5: Additive decomposition of input power density.

of using power input, one can also relate generated electricity to the total rotor swept area. Power output density measures how efficiently the available rotor swept area is used. As explained in section 3, it is the combined effect of the available wind resources (power input density) and the system efficiency. When focusing on land use and its impacts, it makes sense to analyze power output per area of land use. When assuming that the distance between turbines is proportional to their rotor diameters, used land area is also proportional to the total rotor swept area, neglecting effects at the borders of wind parks. Our results of a declining trend in power output density, is therefore in accordance with results by Miller et al. [16, 17] who show that power output per land use is decreasing. Specific power is the ratio between capacity and rotor swept area, that means it sets the maximum electricity generation in relation to the available rotor swept area. Opposed to all previously discussed measures of efficiency, which are related to area and wind resources, economic measures of efficiency show an increasing trend. Capacity factors increased in the period 2010–2019 as shown in Figure A.7. Since the generator size is one of the most important cost factors when building wind turbines [18], this can be seen as main reason for decreasing LCOE. Hence, when interpreting capacity factors as measure of efficiency, capacity relates to costs and represents the input in the relation between output and input. In contrast, in specific power, capacity stands for the output as it is the maximum power output. Note that LCOE is typically defined as costs per amount of energy, but to make it comparable to other measures of efficiency, the reciprocal of LCOE, energy output per costs, is used here.

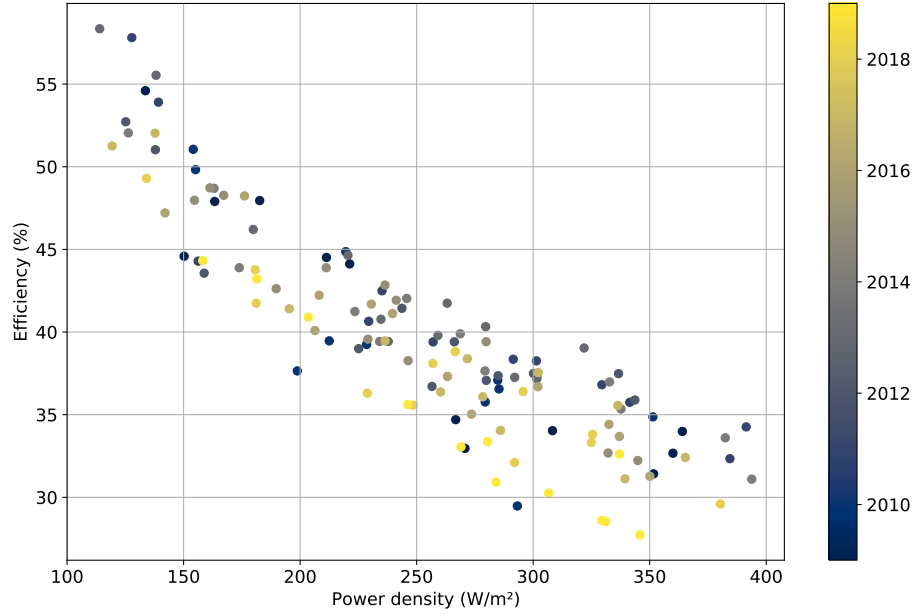


Fig. A.6: Correlation between system efficiency and input power density of monthly aggregated values.

The average coefficient of power

$$\overline{C_p} = \frac{1}{|L|} \sum_{l \in L} \frac{1}{|T|} \sum_{t \in T} C_p(v)$$

is a very similar measure to the system efficiency. System effects, such as wake effects and maintenance, are not included here. Furthermore, $\overline{C_p}$ is an average of ratios and not a ratio of averages (see section A.4.1). The average coefficient of power can be interpreted as the average efficiency of an average wind turbine. However, system efficiency can be interpreted as the efficiency of the total wind power production of all installed wind turbines.

In all discussed definitions of efficiency, measures of produced energy are used. Therefore, the intermittent nature of renewable energy sources is not taken into account. Variability of wind power generation and its correlation with power market prices are of course also important parameters when studying energy systems with high shares of renewables, which are disregarded in the presented efficiency measures.

Table A.1 summarizes the discussed alternative measures of efficiency.

Measure of efficiency	Definition	Unit	Trend	Reference
System efficiency	$\frac{P_{\text{out}}}{P_{\text{in}}}$	dimensionless	decreasing	Section 3.1
Power output density	$\frac{P_{\text{out}}}{A}$	W/m ²	decreasing	Section 3
Power output per land use	$\frac{P_{\text{out}}}{A_{\text{land}}}$	W/m ²	decreasing	[16, 17]
Specific power	$\frac{\text{capacity}}{A}$	W/m ²	decreasing	[18]
Capacity factors	$\frac{P_{\text{out}}}{\text{capacity}}$	dimensionless	increasing	Figure A.7
LCOE (reciprocal)	$\frac{P_{\text{out}}}{\text{costs}}$	Wh/\$	increasing	[18, 31, p. 58]
Average coefficient of power $\overline{C_p}(v)$	$\frac{1}{ V } \sum_{v \in V} \frac{p_{\text{out}_i}(v)}{p_{\text{in}_i}(v)}$	dimensionless	unknown	-

Tab. A.1: Overview of alternative definitions of efficiency.

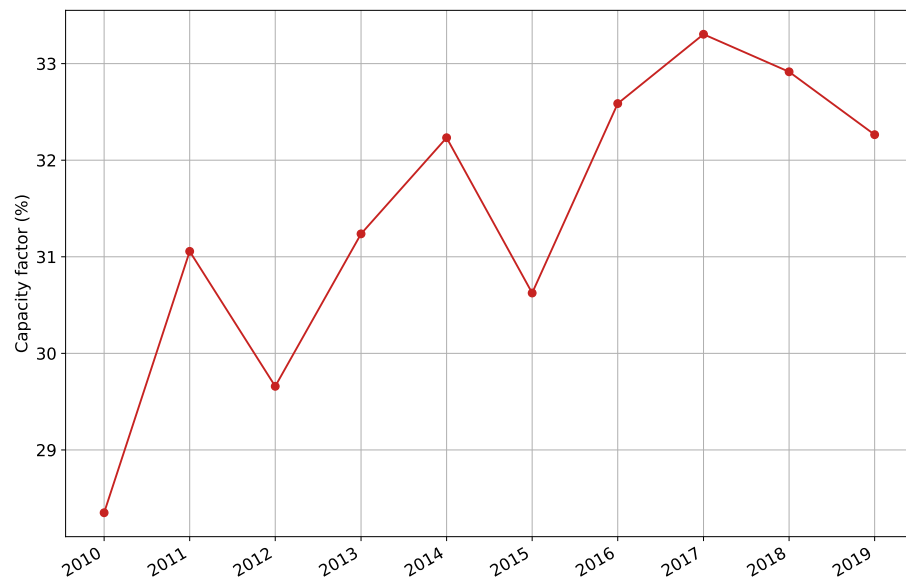


Fig. A.7: Capacity factors for US wind turbines: ratio of total power output and total installed capacity. Note that this is not the average capacity factor as discussed in section A.4.1.